

ABSORBED DOSE ASSESSMENT IN PARTICLE-BEAM IRRADIATED METAL-OXIDE AND METAL-NONMETAL MEMRISTORS

by

***Ivan D. KNEŽEVIĆ¹, Nevena S. ZDJELAREVIĆ¹,
Marija D. OBRENOVIĆ², and Miloš Lj. VUJISIĆ²***

¹Public Company “Nuclear Facilities of Serbia”, Belgrade, Serbia

²Faculty of Electrical Engineering, University of Belgrade, Belgrade, Serbia

Scientific paper
DOI: 10.2298/NTRP1203290K

Absorbed dose was estimated after Monte Carlo simulation of proton and ion beam irradiation on metal-oxide and metal-nonmetal memristors. A memristive device comprises two electrodes, each of a nanoscale width, and a double-layer active region disposed between and in electrical contact with electrodes. Following materials were considered for the active region: titanium dioxide, zirconium dioxide, hafnium dioxide, strontium titanium trioxide and gallium nitride. Obtained results show that significant amount of oxygen ion – oxygen and nonmetal ion – nonmetal vacancy pairs is to be generated. The loss of such vacancies from the device is believed to deteriorate the device performance over time. Estimated absorbed dose values in the memristor for different constituting materials are of the same order of magnitude because of the close values of threshold displacement energies for the investigated materials.

Key words: memristor, proton beam, ion beam, Monte Carlo simulation, absorbed dose

INTRODUCTION

In space applications and in nuclear facility ambience, electronic circuits are under constant bombardment by radiation such as energetic electrons, protons and heavy ions that can upset them or permanently degrade their performance [1]. These particles can ionize atoms in a material, creating a pulse of electron-hole pairs that can cause inadvertent signals in circuit. In addition, energetic particles cause atomic displacement damage in a device which can generate deep traps in a material that lead to carrier removal or mobility degradation [1]. Therefore, it is important to investigate changes of characteristics and the behavior of the electronic components in radiation field.

The properties of basic electrical circuits, constructed from three ideal elements, a resistor, a capacitor, an inductor and an ideal voltage source are part of the standard curricula. The existence of the memristor as the fourth ideal circuit element was predicted in 1971 based on symmetry arguments. In 2008, a two-terminal physical realization of a memristor was constructed by HP laboratories [2]. Exposure of a titanium dioxide memristor to beam of ions can influence the

device's operation [3, 4]. The aim of this paper is to assess the absorbed dose in particle-beam irradiated metal-oxide and metal-nonmetal memristors.

A memristive device comprises at least two electrodes, each of nanoscale width, and an active region disposed between and in electrical contact with the electrodes (fig. 1), containing a switching material capable of carrying a species of dopants and transporting the dopants under an electrical field [5]. Memristor maintains a non-linear relationship between time integrals of the voltage across its terminals and the cur-

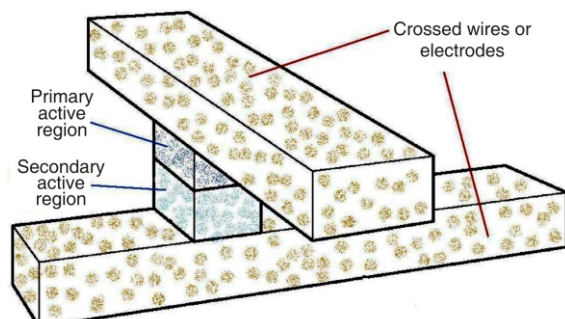


Figure 1. A memristor's structure consisting of crossed wires or electrodes and an active region, divided in two parts – primary and secondary active region [5]

* Corresponding author; e-mail: ivandknezevic@yahoo.com

rent running through it. It is from this non-linear relationship that the main properties of memristors ensue: the hysteretic features of the i-v curve and the ability to operate as a switch by holding or remembering the value of resistance [3, 4]. Within the active region, oxygen vacancies migrate, and such migration is believed to result in memristive effects. The loss of such vacancies from the device is believed to deteriorate the device performance over time. At least one of the two electrodes is a metal oxide electrode, which is believed to reduce or eliminate the escape of oxygen from the device, thus keeping the stoichiometry of the junction constant [5].

The primary active region is a thin film of a material that is electrically semiconducting or nominally electrically insulating and is a weak ionic conductor that can be doped with electron donors as interstitials, vacancies, or impurities. This region is capable of transporting and hosting ions that act as dopants to control the flow of electrons through the structure described. The basic mode of operation of the device is to apply an electrical field across the device large enough to cause mobile dopants to be transported within the primary active region via ionic transport. The mobile dopants are generally ionic species that change electrical conductivity of this region from low to high, and opposite [5].

The secondary active region is a material that acts as a source and sink of the doping species. As a limiting example of forming the secondary active region, dopant initiators may be diffused from a region or source into the primary active region where they react with a portion (a few nanometers or less) of the primary active region. The chemical reaction forms the secondary active region having the mobile dopants therein at the interface between the remaining primary active region and the electrode. Non-limiting examples of dopants that result from the chemical reaction include interstitials, vacancies or other charged impurities. Such mobile dopants are either positively or negatively charged. In one non-limiting example, titanium may diffuse through platinum electrode and react with titanium dioxide (primary active region). This chemical reaction causes the reduction of a portion of the metal oxide, resulting in the formation of a TiO_{2-x} secondary active region at the interface between the remaining titanium dioxide primary active region and the platinum electrode. This TiO_{2-x} secondary active region has a small deficit of oxygen atoms in the crystal structure, or mobile dopants [5].

CONSTITUTING MATERIALS

Non-limiting examples of suitable metal oxides for the metal oxide electrodes include RuO_2 , IrO_2 , $SrRuO_3$, Ce_2O_3 , MoO_2 , OSO_2 , WO_2 , CrO_2 , metallic manganites, and rare earth metal oxides (*e. g.* EuO_x).

The selection of particular metal oxide will depend, at least in part, on the selection of the materials for the active region. The incorporation of such metal oxide electrode in the device advantageously blocks oxygen from escaping out of the device, thereby enhancing device performance and lifetime [5]. If the amplitude of the applied voltage is high enough, oxygen ions may reach one of the electrodes, where they can form O_2 gas and cause deformation of oxide/metal interface, leading to permanent disruption of memristor operation [6].

Possible switch compounds for the primary active region are semiconducting compounds with significant ionic contribution to the bonding. In a non-limiting example, the primary active region is a material that is undoped and stoichiometric, and thus a good insulator and the mobile dopant is a large concentration of anion or cation vacancies contained in the secondary active region, which is a layer of the same material as, or related material to the primary active region. Basically, the secondary active region having the mobile dopants therein is very conductive and thus changing the doping concentration has a relatively small effect on the conductivity of this layer; but since the primary active region is essentially intrinsic, even a small amount of mobile dopant will have a very dramatic effect on the conductivity of this region [5].

In one embodiment, the material of primary active region is selected from oxides, sulfides, selenides, nitrides, phosphides, arsenides, chlorides, and bromides of the transition and rare earth metals, with the alkaline earth metals often being present in compounds. Further, there are the various alloys of like compounds with each other, which offer a wide range of compositions if they are mutually soluble in each other. There are also mixed compounds, in which there are two, three or more different metal atoms combined with some number of the electronegative elements. In such instances, the mobile dopants in the secondary active region may be anion vacancies or different valent elements [5].

Materials for the primary active region including the elements Ti, Zr, and Hf are particularly attractive because they are compatible with Si integrated circuit technology, since the primary oxidation state of all three metals is +4, the same as Si. As such, these elements would not create unintentional doping of the Si. Oxides of these compounds are also known as titania, zirconia, and hafnia, respectively, and also by other names specific to the various polytypes of each. Still another embodiment includes the alloys of these three oxides in pairs or with all three present simultaneously (*e. g.*, $Ti_xZr_yHf_zO_2$, where $x+y+z=1$). Related sets of compounds include the titanates, zirconates and hafnates, which are represented by the specific example $SrTiO_3$, where Sr is the divalent element strontium. There is a wide variety of such compounds in which Ca, Ba, and other divalent elements (*e. g.*, Mg, Zn, Cd)

may be substituted for Sr, and Zr and Hf substituted for Ti. These compounds may be represented as ABO_3 compounds, where A is at least one divalent element and B is at least one of Ti, Zr, and Hf, and may have the perovskite structure [5].

Yet another embodiment of compounds suitable for the primary active region includes the sulfides and selenides of the transition metals with some ionic bonding character, essentially the S and Se analogues of the oxides mentioned above. Still another embodiment of compounds suitable for the primary active region includes the semiconducting halides (such as CuCl, CuBr, and AgCl), or the phosphides and arsenides of various transition and rare earth metals, e. g., Sc, Y, La, etc. In each of the examples set forth in this paragraph, either anion vacancies or aliovalent elements may be used as the mobile dopants in the secondary active region [5]. Specific examples of the combination of primary active regions and secondary active regions are set forth in tab. 1.

Table 1. Examples of primary and secondary active regions and corresponding mobile dopants

| Primary active region | Secondary active region | Mobile dopant |
|-----------------------|-------------------------|--|
| TiO_2 | TiO_{2-x} | Oxygen vacancies or metal interstitials |
| ZrO_2 | ZrO_{2-x} | Oxygen vacancies or metal interstitials |
| HfO_2 | HfO_{2-x} | Oxygen vacancies or metal interstitials |
| SrTiO_3 | SrTiO_{3-x} | Oxygen vacancies or metal interstitials |
| GaN | GaN_{1-x} | Nitrogen vacancies |
| CuCl | CuCl_{1-x} | Chlorine vacancies or copper interstitials |
| GaN | GaN:S | Sulfide ions |

RESULTS OF RADIATION TRANSPORT SIMULATION AND ABSORBED DOSE ASSESSMENT

Monte Carlo simulations of proton and ion beams traversing the selected memristor structures were performed in the TRIM (transport of ions in matter) part of the SRIM software package, which has been proved to provide results in significant agreement with experiments. The constant upgrading development of this software has made it a reliable tool for numerical analysis of interaction of ions with matter and validation of theoretical predictions [7-9]. TRIM is often used to gain an understanding of the changes to the target under bombardment by ions. It makes calculations for one ion at a time, in order to make precise evaluations of the physics of each encounter between the ion and a target atom. Results obtained from TRIM calculations have uncertainties comparable to or lower than typical measurement un-

certainties of results acquired in laboratory experiments performed under corresponding conditions [10, 11]. TRIM can be used for detailed examination of target damage, but it must be interpreted with two limitations: (1) There is no build-up of ions or damage in the target. Every ion is calculated with the assumption of a zero dose, i. e. the target is perfect and previous ions have no effect on subsequent ions. If build-up of damage in the target were included, absorbed dose in the structure would be changed insignificantly since incident ions lose their energy primarily through collisions with non-displaced atoms in the crystal lattice; (2) The target temperature is 0 K and there are no thermal effects changing the distribution of ions (thermal diffusion) or affecting the target damage (thermal annealing). A calculation for 1000 incident ions will give better than 10% accuracy [7]. Several experiments have been reported at very low temperatures (15-40 K) which validate the TRIM results [7]. Detailed modeling of annealing in irradiated memristors needs to be founded on a chemical reaction scheme taking into account evolution rates and diffusion properties of radiation induced defects, which is an area for further research [3].

In order to obtain more detailed information, in the setup window of TRIM software the *Detailed Calculation with Full Damage Cascades* option was chosen as a type of TRIM calculation. TRIM software package enables us to follow history of each particle in the material. The target material is divided into one hundred equal compartments, and in each of these compartments is possible to get final numerical values for the ions and the recoiling target atoms. The output files contain data for each of those parts regarding deposited energy in the material, which includes ion's energy losses to the target electrons, phonons, vacancy production and replacement collisions. These data, together with structure's dimensions and density of the material have been used in order to calculate the value of the absorbed dose in the memristor.

Upon the discussion in the previous section, the following materials were used for the primary-secondary active region structure: $\text{TiO}_2\text{-TiO}_{2-x}$, $\text{ZrO}_2\text{-ZrO}_{2-x}$, $\text{HfO}_2\text{-HfO}_{2-x}$, $\text{SrTiO}_3\text{-SrTiO}_{3-x}$, and GaN-GaN_{1-x} . Platinum was used as a material for metal electrode and RuO_2 was set up for the metal oxide electrode. The thicknesses of the layers along the horizontal axis, for all the structures, are as follows: 3 nm platinum layer, 15 nm primary active region, 15 nm secondary active region ($x = 0.05$), and 3 nm for the second electrode (RuO_2) layer. The default values of the threshold displacement energies provided by SRIM were changed to the following values obtained by different studies: for TiO_2 – threshold displacement energy of 65 eV for oxygen and 130 eV for titanium [4], for ZrO_2 – 50 eV for oxygen and 100 eV for zirconium [12], for HfO_2 – 40 eV for oxygen and 40 eV

for hafnium [13], for SrTiO_3 – 50 eV for oxygen, 70 eV for strontium, and 140 eV for titanium [14], and for GaN – 32.4 eV for nitrogen and 73.2 eV for gallium [15]. Instead of a calculated value for the density of $\text{TiO}_{1.95}$ offered by SRIM, a more realistic value of 4.097 g/cm^3 was used [4]. Also, the densities given by the SRIM for the other compounds of the primary active regions are changed to the values given in different studies: ZrO_2 – 5.68 g/cm^3 , ($\text{ZrO}_{1.95}$ – 5.64 g/cm^3), HfO_2 – 9.70 g/cm^3 , ($\text{HfO}_{1.95}$ – 9.66 g/cm^3), SrTiO_3 – 5.12 g/cm^3 , ($\text{SrTiO}_{2.95}$ –

5.09 g/cm^3), and for GaN – 6.15 g/cm^3 , ($\text{GaN}_{0.95}$ – 6.10 g/cm^3).

Extensive simulations were conducted during the investigation, with ions chosen to represent certain well known radiation fields, such as those encountered in the space or nuclear facility environments [16]. Simulations are restricted to mono-energetic unidirectional beams of radiation, incident perpendicularly on the both sides of the stack of materials constituting the memristor. Beam energy was varied across the typical energy spectrum of different ion species [3]. The MatLab code has been developed in order to obtain the

Table 2. Absorbed dose assessment in different memristor structures

| The structure of irradiated memristor | Type of the beam | | | | | | | |
|--|--|------|--|----|--|-----|---|------|
| | Protons, energy: 10 keV, 1000 particles | | Alpha particles, energy: 100 keV, 1000 particles | | Carbon ions, energy: 100 keV, 1000 particles | | Iron ions, energy: 20 keV, 50 particles | |
| | Absorbed dose in whole memristor [10^4 Gy] | | | | | | | |
| | I* | II** | I | II | I | II | I | II |
| Pt-TiO ₂ -TiO _{1.95} -RuO ₂ | 0.9 | 1.2 | 0 | 0 | 0.4 | 1.9 | 87.7 | 54.7 |
| Pt-ZrO ₂ -ZrO _{1.95} -RuO ₂ | 1.9 | 1.9 | 0 | 0 | 0.4 | 0 | 84.3 | 62.5 |
| Pt-HfO ₂ -HfO _{1.95} -RuO ₂ | 3.2 | 2.5 | 0 | 0 | 1.6 | 0.5 | 141.6 | 64.6 |
| Pt-SrTiO ₃ -SrTiO _{2.95} -RuO ₂ | 2.1 | 2.1 | 0 | 0 | 0 | 0.8 | 133.1 | 53.3 |
| Pt-GaN-GaN _{0.95} -RuO ₂ | 0.8 | 1.9 | 0 | 0 | 0.82 | 0.4 | 92.3 | 62.7 |

I* – Beam perpendicular to the platinum electrode; II** – Beam perpendicular to the RuO₂ electrode

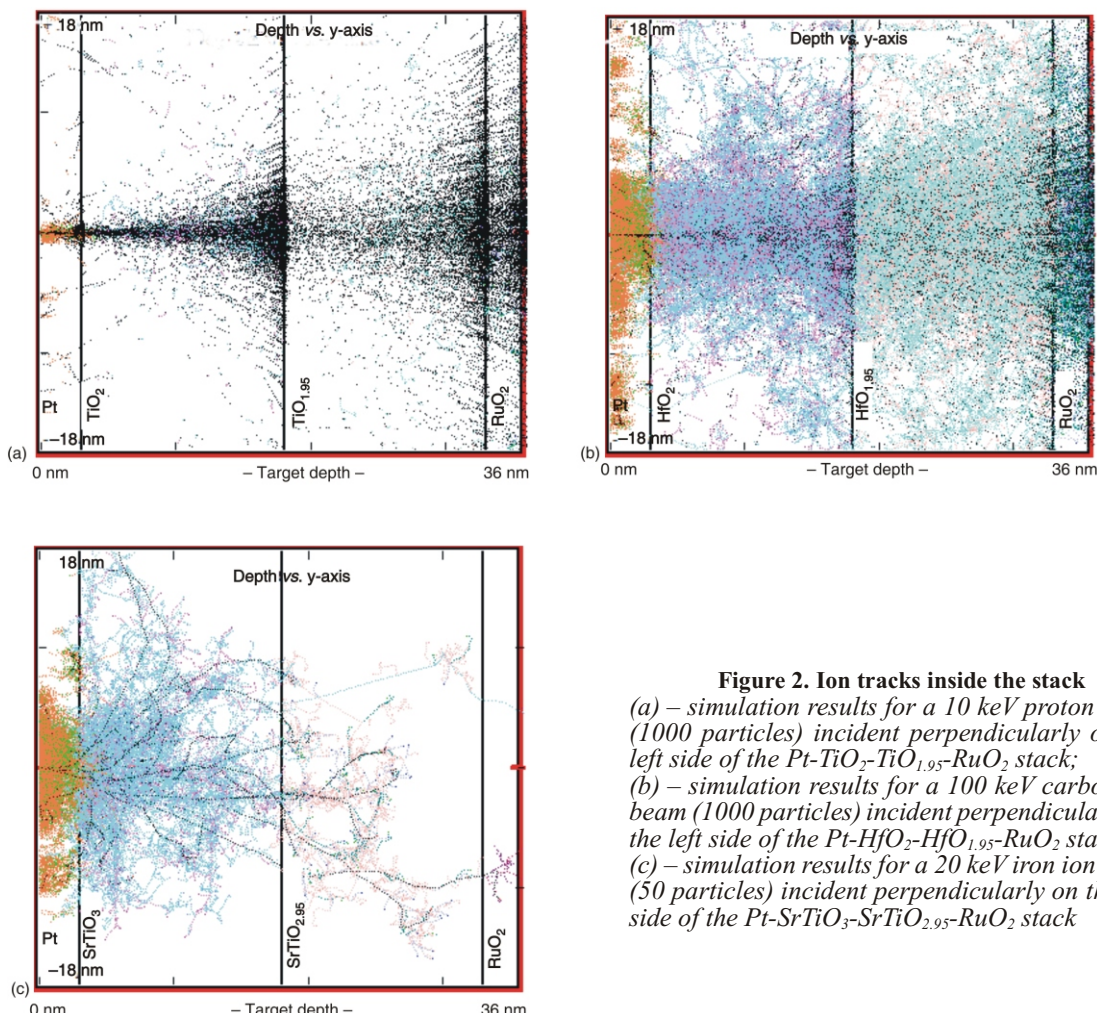


Figure 2. Ion tracks inside the stack
 (a) – simulation results for a 10 keV proton beam (1000 particles) incident perpendicularly on the left side of the $\text{Pt}-\text{TiO}_2-\text{TiO}_{1.95}-\text{RuO}_2$ stack;
 (b) – simulation results for a 100 keV carbon ion beam (1000 particles) incident perpendicularly on the left side of the $\text{Pt}-\text{HfO}_2-\text{HfO}_{1.95}-\text{RuO}_2$ stack;
 (c) – simulation results for a 20 keV iron ion beam (50 particles) incident perpendicularly on the left side of the $\text{Pt}-\text{SrTiO}_3-\text{SrTiO}_{2.95}-\text{RuO}_2$ stack

absorbed dose in the material. The results are shown in the tab. 2.

Figure 2 shows ion tracks traversing the memristor's structure. Figure 2(a) shows simulation results for a 10 keV proton beam incident perpendicularly on the left side of the Pt-TiO₂-TiO_{1.95}-RuO₂ stack. Figure 2(b) shows simulation results for a 100 keV carbon ion beam incident perpendicularly on the left side of the Pt-HfO₂-HfO_{1.95}-RuO₂ stack. Figure 2(c) shows simulation results for a 20 keV iron ion beam incident perpendicularly on the left side of the Pt-SrTiO₃-SrTiO_{2.95}-RuO₂ stack.

Figure 3 shows simulation results for a 10 keV proton beam (1000 particles) incident perpendicularly on the left side of the Pt-GaN-GaN_{0.95}-RuO₂ stack, with a total thickness of 36 nm. Figure 3(a) shows 3-D target damage (total displacements). Figure 3(b) presents 3-D H ion distribution in the material.

Figure 4 presents distribution of displaced oxygen and nitrogen atoms in the material. Figures (a)-(e) show simulation results for proton, alpha particle, carbon ion, iron ion and again proton beam incident perpendicularly on the left side of the following stacks: Pt-TiO₂-TiO_{1.95}-RuO₂, Pt-ZrO₂-ZrO_{1.95}-RuO₂, Pt-HfO₂-HfO_{1.95}-RuO₂, Pt-SrTiO₃-SrTiO_{2.95}-RuO₂ and Pt-GaN-GaN_{0.95}-RuO₂, respectively.

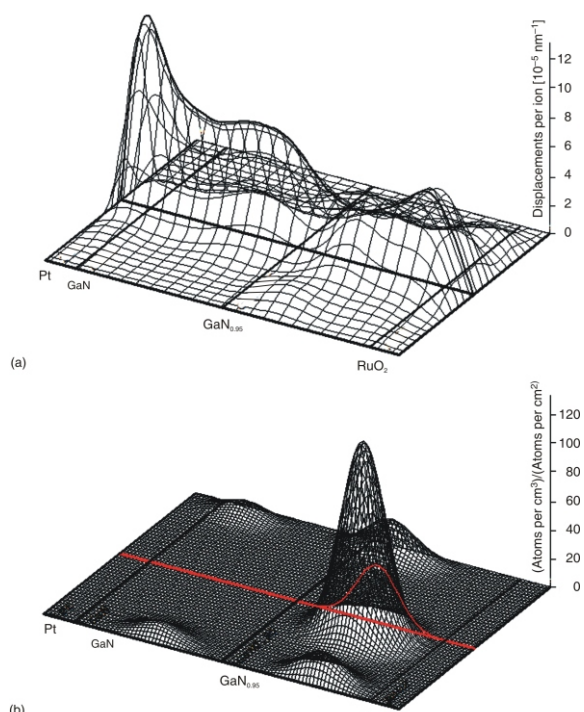


Figure 3. Simulation results for a 10 keV proton beam (1000 particles) incident perpendicularly on the left side of the Pt-GaN-GaN_{0.95}-RuO₂ stack, with a total thickness of 36 nm
(a) – 3-D target damage – total displacements per ion per nm, and
(b) – H ion distribution

DISCUSSION

As Monte Carlo simulations of ion transport show, said radiations can generate a significant amount of oxygen ion/oxygen vacancy pairs in both primary and secondary active regions of the investigated memristor structures. Based on the obtained figures after the simulation process, for a corresponding irradiation beam, a similar distribution of the displaced oxygen and nitrogen atoms is to be found in TiO₂, ZrO₂, and GaN based memristor structures fig. 4(a), (b), and (e). The distribution of displaced oxygen atoms in HfO₂ based structure is more constant throughout the whole material fig. 4(c). There has been noticed a large number of metal atoms (Ti, Zr, Hf, Sr, Ga) displacements throughout the oxide. Primary displaced metal and oxygen atoms cause further displacements that can produce a displacement tree [17, 18]. Primary knock-on atoms with energy less than 2 keV result in isolated defects. Although there is a small number of nuclear elastic and inelastic reaction events that produces cascades, those events are far more damaging and can contribute a significant fraction of the total displacement damage at higher beam energies. Recoils with energies between about 2-10 keV produce single cascades, whereas those with energies in excess of 12-20 keV form a tree-like structure with branches containing multiple cascades [19]. Due to nanometer size of the memristor, this structure is immune to ions with energies greater than 10 MeV [20]. The non-ionizing energy loss (NIEL) of these high energy ions is significantly lower and they cross the volume of the device along almost straight trajectories with proportionally less displacements. For the energy ranges and materials used in simulations, dominant mode of energy loss for charged particles (*i.e.* ions) is ionizing energy loss. Charged particles undergo a well defined “continuous slowing down” energy loss by coulombic interaction with the electron cloud in the lattice, as opposed to uncharged photons and neutrons which undergo a statistically more varied and widely-separated number of scattering events [16]. For the investigated beams and materials, only in the case of iron ions the contribution to the absorbed dose is equally based on non-ionizing and ionizing energy loss. NIEL affects memristor more significantly because investigated component's operation rests upon mobility and concentration of vacancies and ions, which are perturbed by NIEL.

The assessed absorbed dose is of the same order of magnitude for different constituting materials of described memristor structures under the influence of chosen types of particle beams. The contribution to the absorbed dose inside the structure due to influence of alpha particles is zero because the alpha particles are stopped by platinum or RuO₂ electrode. It was expected that the other values obtained for the absorbed dose are of the same order of magnitude because the

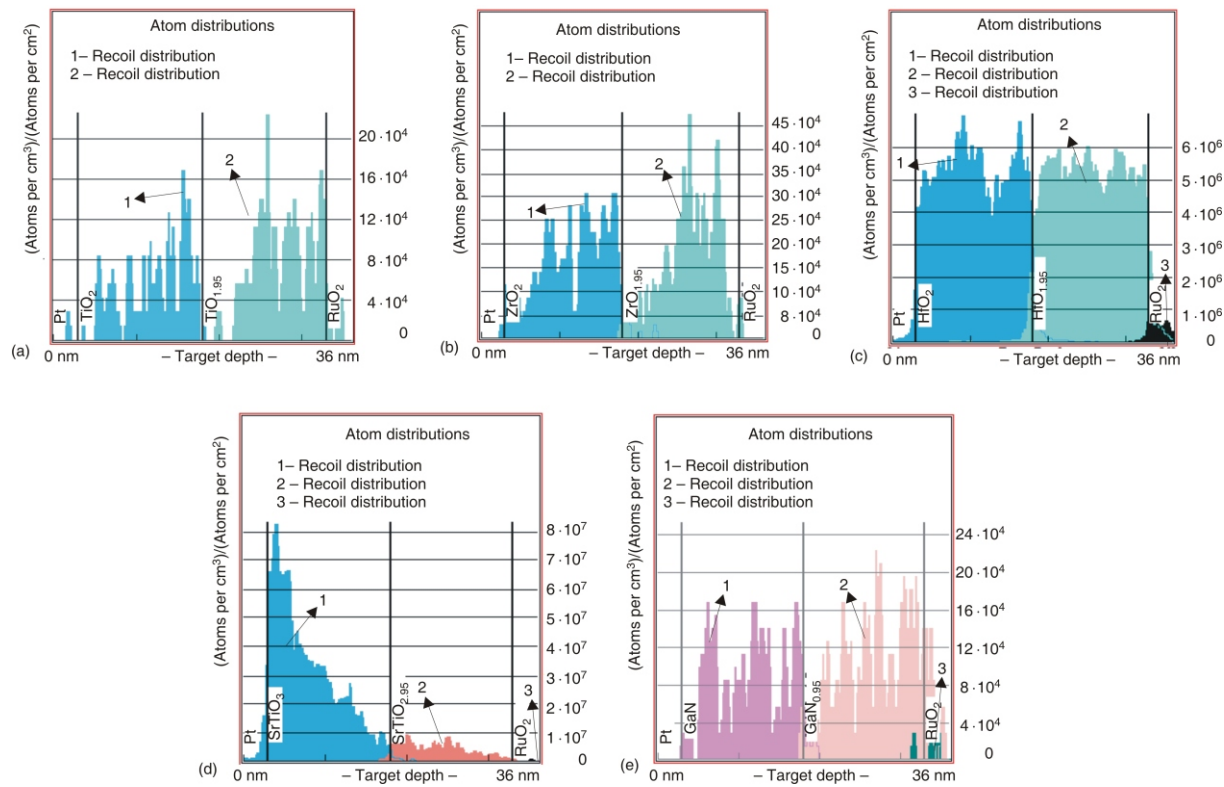


Figure 4. Distribution of displaced oxygen atoms; total thickness of the structure is 36 nm

(a) – simulation results for a 10 keV proton beam (1000 particles) incident perpendicularly on the left side of the Pt-TiO₂-TiO_{1.95}-RuO₂ stack, (b) – simulation results for a 100 keV alpha particle (1000 particles) beam incident perpendicularly on the left side of the Pt-ZrO₂-ZrO_{1.95}-RuO₂ stack, (c) – simulation results for a 100 keV carbon ion beam (1000 particles) incident perpendicularly on the left side of the Pt-HfO₂-HfO_{1.95}-RuO₂ stack, (d) – simulation results for a 20 keV iron ion (50 particles) beam incident perpendicularly on the left side of the Pt-SrTiO₃-SrTiO_{2.95}-RuO₂ stack, and (e) – distribution of displaced nitrogen and oxygen atoms – simulation results for a 10 keV proton beam (1000 particles) incident perpendicularly on the left side of the Pt-GaN-GaN_{0.95}-RuO₂ stack

threshold displacement energies for the investigated metals are between 40 eV and 140 eV.

If the amplitude of the applied voltage is high enough, oxygen ions may reach one of the electrodes where they can form the O₂ gas and cause the deformation of the oxide/metal interface, leading to permanent disruption of memristor operation [6]. Therefore, at least one of the two electrodes is a metal oxide electrode, which is believed to reduce or eliminate the escape of oxygen from the device.

It is important to conduct further investigation in order to choose suitable materials that have necessary radiation tolerance for the required purpose. It is also necessary to design in margins or allowances for the expected component changes induced by the radiation environment.

CONCLUSIONS

Exposure of described types of memristor structure to beams of ions can influence the operation of the

device. Over time, exposure to energetic particles can degrade device performance, ultimately leading to component failure. As Monte Carlo simulations show, a significant amount of oxygen ion/oxygen vacancy pairs are to be generated. This is especially important in primary active region because the appearance of oxygen vacancies in the primary active region can cause its resistance to drop. The absorbed dose in the structure is of the same order of magnitude for all different materials. The contribution to the absorbed dose inside the structure due to influence of alpha particles is zero because the alpha particles are stopped by the electrode. At the end, if the displaced oxygen ions reach the electrode, they can form the O₂ gas and cause a permanent disruption of memristor functionality.

REFERENCES

- [1] William, M. T., et al., Radiation Hardness of TiO₂ Memristive Junctions, *IEEE Transactions on Nuclear Science*, 57 (2010), 3, pp. 1640-1643
- [2] Strukov, D. B., et al., The Missing Memristor Found, *Nature*, 453 (2008), 7191, pp. 80-83

- [3] Vujisić, M., et al., Simulated Effects of Proton and Ion Beam Irradiation on Titanium Dioxide Memristors, *IEEE Transactions on Nuclear Science*, 57 (2010), 4, pp. 1798-1804
- [4] Marjanović, N., et al., Simulated Exposure of Titanium Dioxide Memristors to Ion Beams, *Nucl Technol Radiat*, 25 (2010), 2, pp. 120-125
- [5] Bratovski, et al., Memristive Device, United States Patent, US 7,985,962 B2, 2011
- [6] Yang, J. J., et al., Memristive Switching Mechanism for Metal/Oxide/Metal Nanodevices, *Nat. Nanotechnol.*, 3 (2008), 7, pp. 429-433
- [7] Ziegler, J. F., Biersack, J. P., Ziegler, M. D., SRIM (The Stopping and Range of Ions in Matter), Available online: <http://www.srim.org>
- [8] Warner, J. H., et al., Displacement Damage Correlation of Proton and Silicon Ion Radiation in GaAs, *IEEE Trans. Nucl. Sci.*, 52 (2005), 6, pp. 2678-2682
- [9] Stevens, A. A. E., et al., Amorphous Silicon Layer Characteristics During 70-2000 eV Ar⁺-Ion Bombardment of Si(100), *Journal of Vacuum Science & Technology A: Vacuum, Surfaces, and Films*, 24 (2006), 5, pp. 1933-1940
- [10] Vujisić, M., Stanković, K., Osmokrović, P., A Statistical Analysis of Measurement Results Obtained from Nonlinear Physical Laws, *Applied Mathematical Modeling*, 35 (2011), 7, pp. 3128-3135
- [11] Stanković, K., et al., Statistical Analysis of the Characteristics of Some Basic Mass-Produced Passive Electrical Circuits Used in Measurements, *Measurement*, 44 (2011), 9, pp. 1713-1722
- [12] Edmondson, P. D., et al., Determination of the Displacement Energies of O, Si, and Zr under Electron Beam Irradiation, *Journal of Nuclear Materials*, 422 (2012), 1-3, pp. 86-91
- [13] Usov, I. O., et al., Irradiation Effects in an HfO₂/MgO/HfO₂ Tri-Layer Structure Induced by 10 MeV Au Ions, *Nuclear Instruments and Methods in Physics Research, B* 267 (2009), 11, pp. 1918-1923
- [14] Thomas, B. S., et al., Defects and Threshold Displacement Energies in SrTiO₃ Perovskite Using Atomistic Computer Simulations, *Nuclear Instruments and Methods in Physics Research, B* 254 (2007), 2, pp. 211-218
- [15] Xiao, H. Y., et al., Threshold Displacement Energy in GaN: Ab Initio Molecular Dynamics Study, *Journal of Applied Physics*, 105 (2009), p. 123527 (5)
- [16] Holmes-Siedle, A. G., Adams, L., *Handbook of Radiation Effects*, 2nd ed. Oxford, U.K.: Oxford Univ. Press, 2002, pp. 17-54
- [17] Marjanović, N., et al., Effects of Heavy Ion Bombardment on TiO₂ Memristor Operation, *Radiation Effects and Defects in Solids: Incorporating Plasma Science and Plasma Technology*, 166 (2011), 1, pp. 1-7
- [18] Vujisić, M. Lj., et al., Simulated Radiation Effects in the Superinsulating Phase of Titanium Nitride Films, *Nucl Technol Radiat.*, 26 (2011), 3, pp. 254-260
- [19] Srour, J. R., et al., Review of Displacement Damage Effects in Silicon Devices, *IEEE Transactions on Nuclear Science*, 50 (2003), 3, pp. 653-670
- [20] Vujisić, M., et al., Radiation Hardness of COTS EPROMs and EEPROMs”, *Radiation Effects and Defects in Solids: Incorporating Plasma Science and Plasma Technology*, 165 (2010), 5, pp. 362-369

Received on July 30, 2012

Accepted on August 20, 2012

**Иван Д. КНЕЖЕВИЋ, Невена С. ЗДЕЛАРЕВИЋ,
Марија Д. ОБРЕНОВИЋ, Милош Љ. ВУЈИСИЋ**

**ОДРЕЂИВАЊЕ АПСОРБОВАНЕ ДОЗЕ У МЕМРИСТОРИМА НА БАЗИ
МЕТАЛ-ОКСИДА И МЕТАЛ-НЕМЕТАЛ ЈЕДИЊЕЊА НАКОН ИЗЛАГАЊА
ЈОНСКИМ СНОПОВИМА**

У раду се изучавају ефекти излагања мемристора на бази метал-оксида и метал-неметал једињења дејствујући протонском и јонским споновима применом Монте Карло симулације транспорта честица. На основу излазних параметара симулације, одређена је апсорбована доза у материјалу мемристора. Коришћени модел мемристора састоји се од двослојног танког активног региона који је смештен између две електроде. Димензије уређаја су у нано-скали. Коришћени материјали за активни слој мемристора су: титанијум-диоксид, цирконијум-диоксид, хафнијум-диоксид, стронцијум-титанијум-триоксид и галијум-нитрид. Добијени резултати указују да дуж трајекторија јона у материјалу долази до значајног генерисања парова које сачињавају јон кисеоника и кисеонична ваканција, односно јон неметала и ваканција неметала. Губитак ових ваканција из уређаја доводи до погоршавања рада уређаја током времена. Добијене вредности апсорбованих доза у материјалу мемристора за различите конститутивне материјале и за различите типове јонских спонова су истог реда величине због близких вредности енергије прага за измештање атома у датој структури.

Кључне речи: мемристор, јонски спон, Монте Карло симулација, апсорбована доза